JOURNAL OF SYNCHROTRON RADIATION
ISSN 1600-5775

Effect of atomic vibrations in XANES: polarization-dependent damping of the fine structure at the Cu *K*-edge of $(creat)_2CuCl_4$

Ondřej Šipr,[a]* Jiří Vackář[b] and Alexei Kuzmin[c]

[a]Institute of Physics of the ASCR v.v.i., Cukrovarnicka 10, CZ-162 53 Prague, Czech Republic, [b]Institute of Physics of the ASCR v.v.i., Na Slovance 2, CZ-182 21 Prague, Czech Republic, and [c]Institute of Solid State Physics, University of Latvia, Kengaraga Street 8, LV-1063 Riga, Latvia. *Correspondence e-mail: sipr@fzu.cz

Received 2 May 2016
Accepted 13 September 2016

Edited by R. W. Strange, University of Essex, UK

Keywords: XANES; vibrations; multiple-scattering formalism.

Polarization-dependent damping of the fine structure in the Cu *K*-edge spectrum of creatinium tetrachlorocuprate [$(creat)_2CuCl_4$] in the X-ray absorption near-edge structure (XANES) region is shown to be due to atomic vibrations. These vibrations can be separated into two groups, depending on whether the respective atoms belong to the same molecular block; individual molecular blocks can be treated as semi-rigid entities while the mutual positions of these blocks are subject to large mean relative displacements. The effect of vibrations can be efficiently included in XANES calculations by using the same formula as for static systems but with a modified free-electron propagator which accounts for fluctuations in interatomic distances.

1. Introduction

Including vibrations in X-ray absorption spectra (XAS) calculations is in general difficult because in principle one has to evaluate the spectrum for all possible geometric configurations (distributions of instantaneous positions of atoms) and average the signals with proper weights. Doing this explicitly might be computationally very demanding so usually some further simplifications are invoked, such as the assumption of a Gaussian or nearly Gaussian distribution regarding the atomic positions and of the validity of single-scattering and plane-wave approximations regarding the effect of vibrations on the photoelectron state (Beni & Platzman, 1976; Lee *et al.*, 1981).

Dealing with Gaussian or harmonic vibrations for extended X-ray absorption fine structure (EXAFS) calculations is a relatively straightforward procedure, as long as we deal with the energy region where the single-scattering and plane-wave approximations can be used. Here, the main challenge is to find the vibrational modes of the system and to use them for obtaining the appropriate parameters (Dimakis & Bunker, 1998; Poiarkova & Rehr, 1999; Vila *et al.*, 2007; Dimakis *et al.*, 2009). Accurate EXAFS calculations for molecular complexes were published with vibrations included on a truly *ab initio* level (Veronesi *et al.*, 2010; Rega *et al.*, 2011).

The influence of vibrations in the X-ray absorption near-edge structure (XANES) region is expected to be small, as reflected by the Debye–Waller factor $\exp(-2\sigma^2k^2)$ which occurs in the conventional EXAFS formula. However, there might be effects in the XANES or intermediate energy regions for which the vibrations could be important. A good strategy for finding such effects is to focus on polarized spectra of layered systems, because (i) polarized XANES contains

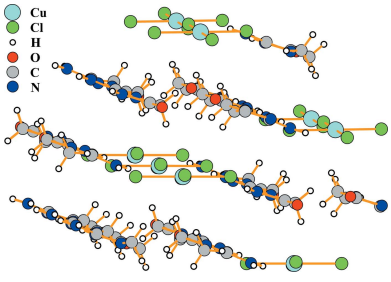

significantly more information than orientationally averaged spectra, meaning also that polarized XANES presents a much more stringent test to the theory, and (ii) for layered systems it is more likely that the vibrations will damp different scattering signals differently, thus giving rise to features in the spectra which might not be possible to explain unless these vibrations are taken into account.

Including vibrations in XANES calculations, where multiple-scattering effects have to be considered, is difficult because, among others, one should deal with displacements of more than just two atoms at a time. One possible direction is to employ a Taylor expansion around equilibrium positions to obtain a usable formula for the statistical average of the signals for different geometric configurations. This approach was pursued by Benfatto *et al.* (1989) who started with analytic formulae describing signals of order n and applied the expansion regarding both the free-electron propagator and the scattering phase shifts. In this way, correlated vibrations of n-atom configurations could be accounted for (Filipponi *et al.*, 1995), as is implemented, for example, in the *GNXAS* code (Cicco, 2003). A formally similar route was taken by Fujikawa *et al.* (1999) who also applied a Taylor expansion but this time regarding only the propagator.

Another possible approach is to rely on scattering path expansion to employ Debye–Waller damping factors specific for each scattering path (Poiarkova & Rehr, 1999). Similarly to the scheme of Benfatto *et al.* (1989), this scheme is more suitable to the EXAFS than to the XANES because it can be used only if the scattering path expansion converges (Rehr & Albers, 2000).

All these procedures have various degrees of accuracy and sophistication and proved to be useful in various circumstances (Loeffen & Pettifer, 1996; Hayakawa *et al.*, 1999, 2003). At the same time, their implementation is not simple. It is noteworthy that, even though methodological works undoubtedly present a significant progress (Benfatto *et al.*, 1989; Dimakis & Bunker, 1998; Fujikawa *et al.*, 1999; Poiarkova & Rehr, 1999; Vila *et al.*, 2007; Dimakis *et al.*, 2009), practical applications to XANES calculations remain rare. A broader use of these techniques could be stimulated by demonstrating that useful results can be obtained even by simple implementations of the procedures mentioned above. If these techniques are to be used in the XANES region, one has to opt for a formulation which treats the multiple scattering exactly. On top of that, it would be convenient if correlations between movements of various atoms were taken into account to some extent. In this work we focus on testing a simplified version of the method of Fujikawa *et al.* (1999), which consists of calculating XANES by using essentially the same formula as for static systems, just with a modified free-electron propagator to account for pair-wise fluctuations of interatomic distances. Effectively this means that the multiple scattering is treated exactly while the effect of vibrations is treated within the plane wave approximation. Respective formulae were already incorporated earlier, for example in the *FEFF9* code (Rehr *et al.*, 2010; Rehr, 2013). However, to the best of our knowledge they have not really been used for solving practical problems of XANES analysis so far. We suggest that by means of the procedure outlined in §2.1 one can describe experimentally observable trends that could not be described within the static lattice model. We demonstrate this in the case of Cu K-edge spectra of creatinium tetrachlorocuprate, $(\text{creat})_2\text{CuCl}_4$.

Copper K-edge XAS of Cu-containing complexes was subject to intensive research in the past. There has been a still unsettled debate about the 'local and many-body' or 'delocalized and one-electron' interpretation of XANES at the Cu K-edge in systems containing CuCl_n or CuO_n blocks (Hahn *et al.*, 1982; Kosugi *et al.*, 1984, 1989; Smith *et al.*, 1985; Yokoyama *et al.*, 1986; Guo *et al.*, 1990; Bianconi *et al.*, 1991; Bocharov *et al.*, 2001; Kosugi, 2002; Chaboy *et al.*, 2006; Calandra *et al.*, 2012). An important place in these discussions was given to the angular or polarization dependence of the spectra close to the edge. However, not much attention has been paid to the polarization dependence of XAFS further above the edge, for photoelectron energies in the range 30–100 eV. A striking feature here is a big difference in how the XAFS oscillations are damped with increasing energy for different polarizations of the incoming X-rays.

We demonstrate in this work that the dependence of the damping of the fine structure on the polarization cannot be explained by calculations which rely on a static lattice. By including vibrations in the XANES calculations we show that the observed anisotropy of XAFS damping can be reproduced if the mean-square relative displacements (MSRDs) are chosen so that individual molecular blocks in the $(\text{creat})_2\text{CuCl}_4$ crystal are treated as semi-rigid entities while the mutual positions of these blocks are subject to large disorder. XANES analysis thus offers a view on the nature of the vibrations in the material in question. The procedure we employ is especially suited for analysing layered systems.

2. Methods

2.1. Treatment of vibrations

The method we use for accounting for the vibrations is essentially the same as that introduced by Fujikawa *et al.* (1999) as 'renormalization of the scattering series by a plane-wave thermal factor'. As mentioned in §1, the formula was also included in the *FEFF9* code (Rehr *et al.*, 2010; Rehr, 2013) but no discussion was given. The procedure consists of calculating the XANES using the same formula as for static systems (Vvedensky, 1992; Natoli *et al.*, 2003; Rehr & Albers, 2000) but replacing the free-electron propagator $G^{pq}_{LL'}$ in the basic multiple-scattering equation according to the *ansatz*

$$G^{pq}_{LL'} \rightarrow G^{pq}_{LL'} \exp\left(-k^2\sigma^2_{pq}\right), \qquad (1)$$

where σ^2_{pq} is the MSRD characterizing the fluctuations of the distance between the atoms p and q.

Thus if one calculates XANES along the same procedures as in the static case with only performing the substitution (1), one obtains the spectrum for a vibrating system, with the full multiple scattering treated exactly and with the effects of the

vibrations treated approximatively. In particular, (i) the effect of vibrations is restricted to changes in the geometry, *i.e.* the scattering phase shifts are the same as for a static system, (ii) the effect of vibrations is restricted to varying the bond lengths for each pair independently, neglecting thus, among others, bond angles variations, and (iii) the effect of vibrations is treated within the plane-wave approximation (while the electron scattering itself and hence the bulk of the spectral shape are calculated exactly, *i.e.* with curved waves). It should be mentioned that correlations between movements of different atomic pairs can be included only partially, by a suitable choice of the MSRD for each pair, as done in §3 below.

We will show in the following that despite all the approximations, the *ansatz* equation (1) can describe the effect of vibrations so that features seen in the experiment can be interpreted as arising from vibrations.

2.2. Technical details of XANES calculations

The crystal structure of $(creat)_2CuCl_4$ is monoclinic (crystal group 14). Lattice vectors lengths used were a = 8.106 Å, b = 7.835 Å, c = 13.685 Å, with angles between the lattice vectors $\alpha = 90°$, $\beta = 114°$, $\gamma = 90°$. The structural diagram is shown in Fig. 1. Most of the calculations presented here were performed within the real-space multiple-scattering formalism, using the *RSMS* code (Šipr, 1996–1999). We used a non-self-consistent muffin-tin potential constructed according to the Mattheiss prescription (superposition of potentials and charge densities of isolated atoms). The core hole left by the excited photoelectron was treated within the final state approximation ('relaxed and screened model') (Vvedensky, 1992; Natoli *et al.*, 2003). The exchange and correlation effects were accounted for *via* the energy-independent $X\alpha$ potential with a Kohn–Sham value of α = 0.67. The XANES spectra were obtained for clusters of radii of 7.8 Å (185 atoms including H atoms, 103 atoms disregarding H atoms). Spectra calculated with H atoms and without H atoms are practically identical.

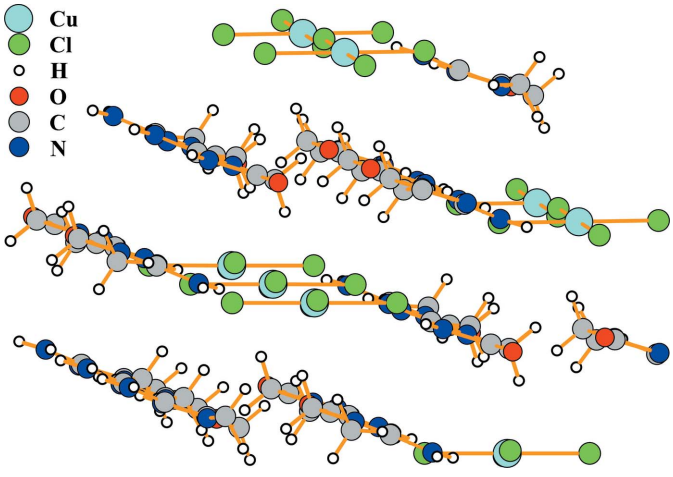

Figure 1
Structural diagram of $(creat)_2CuCl_4$. The z-axis is perpendicular to the $CuCl_4$ blocks.

Raw spectra were broadened by an energy-dependent Lorentzian to simulate the combined effect of the experimental resolution, of the decay of the core hole and of the decay of the excited photoelectron. The constant part of the broadening was set to 1.50 eV; the energy-dependent part of the broadening was set to $0.08E$, where E is the photoelectron energy.

2.3. Plane-waves calculations

Band-structure calculations relying on the plane waves basis set and pseudopotentials were performed using the *ABINIT* code (Gonze *et al.*, 2009). First, a self-consistent calculation was performed using 16 k-points in the irreducible Brillouin zone. Afterwards, the angular-momentum-projected density of states (DOS) within a sphere around the Cu atom with radius of 1.24 Å was calculated using 38 k-points. The cut-off energy for the plane waves was set to 40 Hartree. The core hole was ignored. The results presented here were obtained using a Hartwigsen–Goedeker–Hutter type pseudopotential available at the *ABINIT* web site (Krack, 2005).

Because of the use of pseudopotentials, we did not have access to the core wavefunctions and, consequently, were not able to calculate XANES spectra directly. However, if the core hole is neglected and the dipole selection rule is invoked, polarized XANES spectra can be taken as proportional to the appropriate angular-momentum component of the projected DOS multiplied by a smooth function which corresponds to the square of the atomic transition matrix element M_L. The proportionality between XAS and DOS is, strictly speaking, true only under specific symmetry requirements which guarantee that the scattering path operator is diagonal. However, in most cases this is fulfilled with sufficient accuracy. We checked explicitly using the *RSMS* code that XAS and DOS are indeed proportional in our case. A similar approach was used by Nesvizhskii *et al.* (2001) to obtain DOS from XAS for the sum rules analysis.

Having all this in mind, we obtained XANES *via ABINIT* simply by taking the projected DOS and multiplying it by a smooth sinusoidal-like function which increases monotonously from 1.0 at the absorption edge to 1.6 at the end of the energy region we cover. We chose this particular form of the DOS-to-XAS proportionality function just for convenience; our conclusions are not dependent on it. Polarization sensitivity of the spectra was achieved by taking the ($\ell = 1$, $m = 0$) DOS component to obtain the XANES with the $\varepsilon \parallel z$ polarization and the ($\ell = 1, m = \pm 1$) DOS component to obtain the XANES with the $\varepsilon \perp z$ polarization. The same convolution of the raw results by an energy-dependent Lorentzian curve was applied as in the case of real-space multiple-scattering calculations.

3. Application to the Cu *K*-edge XAS of $(creat)_2CuCl_4$

In the following we will demonstrate that the effect of vibrations can be identified at the Cu K-edge XAS of $(creat)_2CuCl_4$. The experimental spectrum taken from Kosugi *et al.* (1984) is

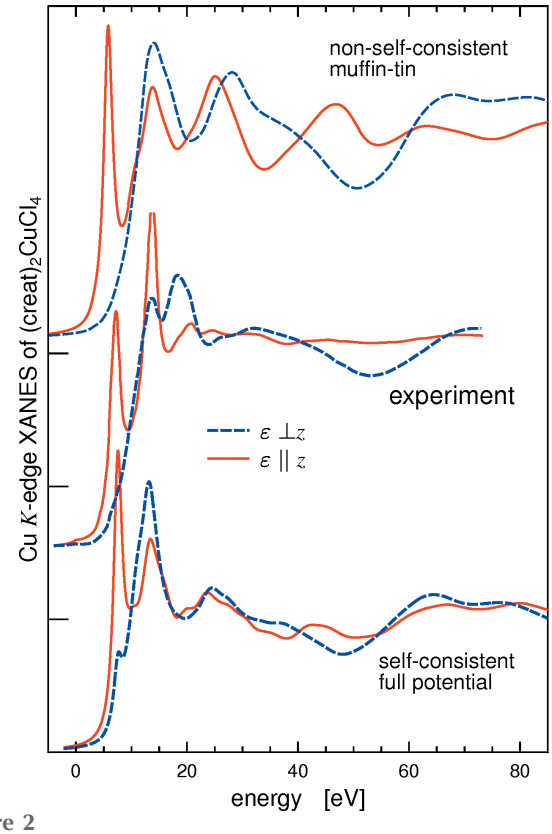

Figure 2
Experimental polarized Cu *K*-edge XANES of $(creat)_2CuCl_4$ (Kosugi *et al.*, 1984) compared with spectra calculated for a static crystal. The uppermost panel displays spectra obtained *via* the *RSMS* code, the lowermost panel displays spectra obtained *via* the *ABINIT* code. The origin of the energy scale is arbitrary.

shown in the second from bottom panel of Fig. 2. The polarization vector of the incoming X-rays either lies in the plane defined by the photoabsorbing Cu atom and its four nearest Cl neighbours ($\varepsilon \perp z$) or is perpendicular to this plane ($\varepsilon \parallel z$, *cf.* Fig. 1). Unlike most of the previous works on the Cu *K*-edge XAS of $(creat)_2CuCl_4$, our focus is not on the first 10 eV above the edge but on the higher-energy region, in particular on the strong suppression of the fine structure for the $\varepsilon \parallel z$ spectrum for energies 20 eV and more above the edge.

3.1. Calculations for a static lattice

First we find out whether the anisotropic damping of XAFS oscillations can be reproduced by calculations carried out for a static crystal. Theoretical XANES obtained using the *RSMS* code are shown above the experimental spectrum in Fig. 2; the spectrum obtained using the *ABINIT* code is shown below the experiment. Spectra labelled $\varepsilon \parallel z$ were calculated for linearly polarized X-rays; spectra labelled $\varepsilon \perp z$ were calculated for circularly polarized X-rays. The horizontal alignment of the spectra was done by hand so that the position of the $\varepsilon \parallel z$ peak around 12 eV matches the experiment. The static effect of the 1*s* core hole as described within the final-state approximation is practically negligible: spectra obtained *via* the *RSMS* code for the potential with the core hole can hardly be distinguished from spectra obtained for the ground-state potential (not shown here).

None of the calculations describes the suppression of the fine structure for $\varepsilon \parallel z$. It is thus evident that the anisotropic damping of XAFS oscillations for energies 20 eV or more above the edge cannot be reproduced by calculations performed for a static $(creat)_2CuCl_4$ crystal.

Concerning individual spectra, our calculations are unable to reproduce correctly the peak intensities within the first 10 eV above the absorption edge. We conjecture that this is connected with many-body effects beyond the local density approximation. Let us recall in this regard the discussion about whether the Cu *K*-edge XANES of complexes containing linear or square-planar $CuCl_n$ units is dominated by many-body (mostly shake-down) features or whether it is dominated by hybridization between states of neighbouring $CuCl_n$ units (Kosugi *et al.*, 1984; Smith *et al.*, 1985; Yokoyama *et al.*, 1986; Kosugi, 2002).

Interestingly, the shape of the broad $\varepsilon \parallel z$ peak around 20–30 eV cannot be described accurately unless a self-consistent full potential is used: the three sub-peaks this feature consists of are well reproduced by *ABINIT* calculations but not by *RSMS* calculations. It appears thus that, disregarding the topic of the anisotropic XAFS damping, the states lying predominantly in the *xy* crystallographic plane, which contains a lot of atoms, are well described by the non-self-consistent muffin-tin potential, while the states in the more-or-less empty interstitial region between the $CuCl_4$ planes can be described properly only if the approximations laid on the potential are relaxed. This is plausible; one expects that the muffin-tin approximation will be more crude in empty regions than in regions packed with atoms.

Finally, we should mention that our theoretical spectra do not exhibit the weak pre-edge structure which appears in the experiment around 0 eV in the scale of Fig. 2 (X-ray energies about 8978 eV). Our calculations are based on the dipole selection rule; the pre-edge structure, on the other hand, is to a large extent formed by quadrupole transitions (Hahn *et al.*, 1982; Bocharov *et al.*, 2001; Wu *et al.*, 2004). Another contribution to the pre-edge structure may come from dipole transitions allowed by vibrational symmetry breaking (Vedrinskii *et al.*, 1998; Manuel *et al.*, 2012). We want to focus rather on the higher-energy part of the spectrum.

3.2. Influence of vibrations

Because static lattice calculations were not able to reproduce the large difference between the damping of XAFS oscillations for the $\varepsilon \parallel z$ and for $\varepsilon \perp z$ polarizations, we performed another set of calculations, accounting this time for vibrations by the method described in §2.1. The occurrence of the anisotropic damping of XAFS in the experiment suggests that one should consider different MSRDs for different bonds. This means that we have to identify which interatomic distances will be regarded as stiff and which will be regarded as soft. By inspecting the $(creat)_2CuCl_4$ structure one can

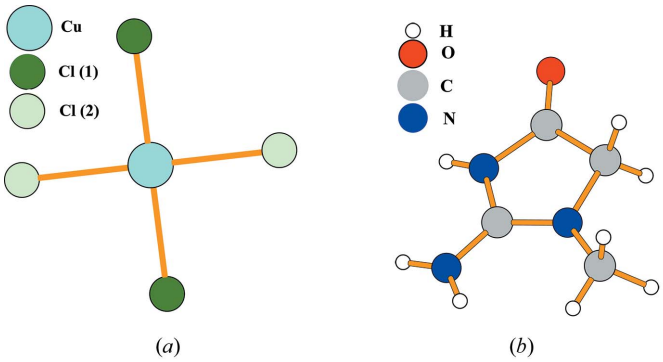

Figure 3
Molecular blocks forming the $(creat)_2CuCl_4$ crystal.

realise that the $(creat)_2CuCl_4$ crystal is actually formed by creatinium and $CuCl_4$ molecular units which are relatively independent (they are linked through N—H···Cl hydrogen bonding) (Udupa & Krebs, 1979). These units are displayed in Fig. 3. We assume that, if two atoms belong to the same molecular unit, then their interatomic distance is characterized by a small MSRD which we denote σ^2_{idd}. If two atoms belong to different molecular units, then their interatomic distance is characterized by a large MSRD, denoted as σ^2_{diff}. At the moment, we have no clear indication of how to choose the values of σ^2_{idd} and σ^2_{diff}, and therefore we treat them as model parameters and set their values in accordance with that reported for other systems in the literature. Our goal is to check whether a model based on the substitution of equation (1) with two distinct σ^2 parameters can simulate the anisotropic XAFS damping which we observe for $(creat)_2CuCl_4$.

We performed a set of calculations with a fixed σ^2_{idd} = 0.0008 Å^2 while varying σ^2_{diff} as 0.008, 0.084 and 0.840 Å^2. These results are compared with results for a static lattice and with the experimental data (Fig. 4). One can see that, if we take σ^2_{diff} = 0.084 Å^2, the XAFS oscillations for the $\varepsilon \parallel z$ component are strongly damped for X-ray energies above 20–30 eV, as required. A substantially lower σ^2_{diff} does not lead to the desired damping while a substantially larger σ^2_{diff} results in overdamping of the oscillations at low energies. We can thus conclude that our way of including the vibrations in the XANES calculations, together with the scheme for assigning σ^2_{idd} and σ^2_{diff} to atomic pairs depending on whether they belong to the same molecular unit or not, is a good approximation for describing the mechanism of the anisotropic damping of XAFS for $(creat)_2CuCl_4$.

4. Discussion

Our goal was to examine whether effects of vibrations can be identified in XANES if the vibrations are included in the theory by modifying the free-electron propagator. By calculating Cu *K*-edge spectra of $(creat)_2CuCl_4$ obtained for static and for vibrating systems we were able to link the differences in the damping of experimental XAFS for the in-plane and out-of-plane polarizations to the differences in MSRDs

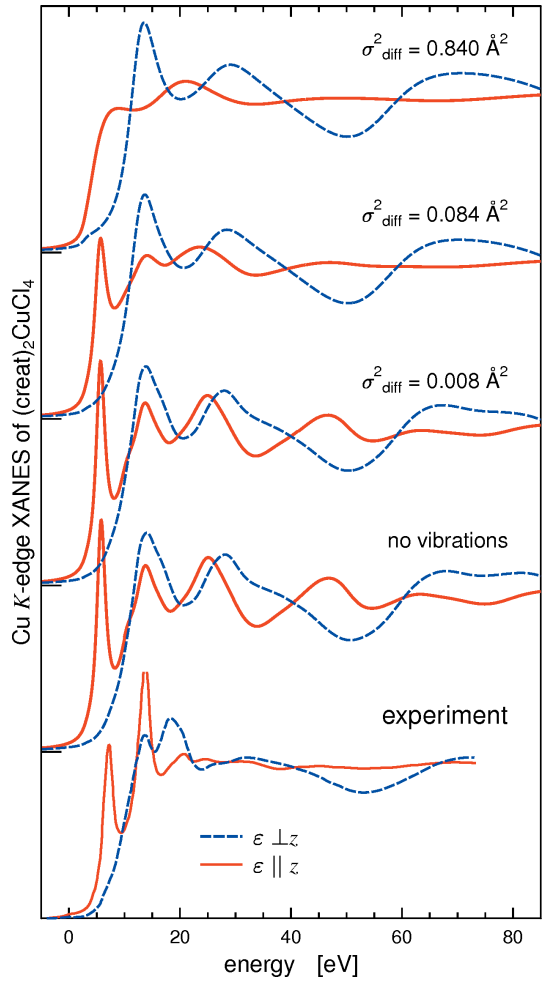

Figure 4
Theoretical Cu *K*-edge XANES of $(creat)_2CuCl_4$ calculated while including the vibrational disorder, compared with the static lattice calculation and with the experiment.

according to whether the respective atoms belong to the same molecular unit or not.

The MSRD values σ^2_{idd} = 0.0008 Å^2 and σ^2_{diff} = 0.084 Å^2 are realistic considering analogous data obtained for similar systems. For example, the MSRD values σ^2(Cu—Cl) = 0.0013–0.0041 Å^2 given by Tanimizu *et al.* (2007) and 0.008 Å^2 by Ivashkevich *et al.* (2008) were obtained for the fourfold Cl coordination of copper in chloro-complexes. Note that in these two cases copper atoms are additionally bonded to two oxygen or nitrogen atoms, located at shorter distances than four chlorine atoms. As a result, the Cu—Cl bonding in chloro-complexes is weaker than the Cu–Cl bonding in $(creat)_2CuCl_4$, and, consequently, the corresponding MSRDs are expected to be larger in chloro-complexes than in $(creat)_2CuCl_4$.

We can also make a comparison with crystallographic data (Udupa & Krebs, 1979). However, one has to bear in mind that in crystallography one deals with disorder in the distribution of atomic displacements measured from a lattice point while in XAS one deals with disorder in the distribution of interatomic distances. Correlations between movements of atoms are responsible for the differences between crystal-

lographic σ^2_{cryst} and XAS-related σ^2_{XAS}. Crystallographic data suggest that the vibrations of all atoms in $(creat)_2CuCl_4$ are strongly anisotropic: σ^2_{cryst} along the z axis is up to four times larger than σ^2_{cryst} within the xy plane (Udupa & Krebs, 1979). This is consistent with our picture, because small 'intra-block' vibrations associated with σ^2_{idd} will be mostly in the xy plane while large 'inter-block' vibrations associated with σ^2_{diff} will be both in the xy plane and along the z axis. If the correlations are neglected, an estimate for pair-wise σ^2_{XAS} can be obtained by summing the crystallographic σ^2_{cryst} values for the respective atom pair (Udupa & Krebs, 1979). If we do this for the Cu–X pairs along the z axis, where only weak correlations can be expected, we obtain $\sigma^2_{XAS} = 0.10$–0.17 Å^2. This is comparable with our $\sigma^2_{diff} = 0.084$ Å^2. For vibrations in the xy plane, σ^2_{cryst} is about 0.05–0.09 Å^2 if no correlations are assumed. This is significantly larger than the σ^2_{idd} we use. However, our assumption of the stiffness of individual molecular blocks means that there should be large correlations between movements of respective atoms, so crystallographic σ^2_{cryst} cannot be directly compared with our σ^2_{idd} in this respect.

While we focus on XANES, large differences between vibration amplitues in different directions were probed earlier by EXAFS for other systems (Yokoyama *et al.*, 1996; Schnohr *et al.*, 2009; Bridges *et al.*, 2014). A lot of attention has focused on this aspect, *e.g.* in connection with negative thermal expansion (Ahmed *et al.*, 2009; Fornasini & Grisenti, 2015).

The way we include the vibrations in XANES calculations has been done before but only to investigate XANES in liquids close to critical conditions and relying on more complicated equations that the simple substitution of equation (1) (Hayakawa *et al.*, 1999, 2003). In this work we focus on a crystal at room temperature and demonstrate that the simple formula (1) can be used to identify vibrational effects in X-ray absorption spectra in the XANES and intermediate energy regions.

The scheme we employed treats the multiple scattering in an exact way but the vibrations in an approximative way. However, we do not expect this to have any significant influence on our conclusions. As concerns the plane-wave approximation laid on the vibrations, it is true that Fujikawa *et al.* (1999) found a difference in XANES calculated when the vibrations were treated within the spherical-wave approximation [equation (3.16) of Fujikawa *et al.* (1999)] and when the vibrations were treated within the plane-wave approximation [equation (3.18), *ibid.*] but this was only for short bond lengths and very large $\sigma^2 = 0.4$ Å. For longer distances, this effect was already very small. In our situation, short bond lengths (between atoms of the same molecular unit) are characterized by small σ^2, while large σ^2 is associated only with large bond lengths. Hence, the plane-wave approximation should be sufficient for the vibrations in this case. As concerns the effect of the vibrations on the scattering phase shifts, the situation is more complicated: earlier studies found some effects in this respect, especially as concerns the higher-order scattering signals (Benfatto *et al.*, 1989; Yokoyama & Ohta, 1996). On the other hand, we do not expect this effect to dominate in our situation, because we found that several different potentials lead to similar results in the energy region where the effect of vibrations are visible.

Our focus is on the very fact that vibrations give rise to significant observable effects in the polarization-dependence of $(creat)_2CuCl_4$ XANES spectra and not on the particular values of σ^2_{idd} and σ^2_{diff}. The approximations involved in the model do not allow for taking our σ^2_{idd} and σ^2_{diff} values as true best fits. Besides, our splitting of the atomic pairs into the σ^2_{idd} and σ^2_{diff} classes is not unique. For example, the σ^2_{idd} and σ^2_{diff} MSRDs could be ascribed to the pairs depending on whether the respective atoms belong to the same layer or not (the layers are depicted in Fig. 1). We performed the calculations also for this model and found that the results are almost the same as for the molecular-units-based model. This is not so surprising because atoms belonging to the same unit belong also to the same layer. We also verified that the particular value of $\sigma^2_{idd} = 0.0008$ Å^2 is not crucial; nearly identical results are obtained with a much larger value of $\sigma^2_{idd} = 0.008$ Å^2. Despite the unavoidable ambiguity, we nevertheless assume that the large difference between σ^2_{idd} and σ^2_{diff} would be maintained even if a more advanced modelling was employed.

Our interpretation that the polarization dependence of the XAFS damping in $(creat)_2CuCl_4$ is a manifestation of the existence of very different MSRDs depending on whether the pair-forming atoms belong to the same basic molecular unit could be confirmed (or refuted) by temperature-dependent measurements of the polarized spectra. If XAFS oscillations for $\varepsilon \parallel z$ are gradually restored when the temperature decreases so that XAFS amplitudes become comparable for $\varepsilon \parallel z$ and $\varepsilon \perp z$, as suggested by static lattice calculations (see Figs. 2 and 4), it would be a strong argument in favour of our interpretation.

5. Conclusions

Fine-structure oscillations in the experimental Cu K-edge XAS of $(creat)_2CuCl_4$ in the near-edge and intermediate energy region are damped differently for in-plane and out-of-plane polarization. The anisotropy of the XAFS damping cannot be reproduced by the theory unless the vibrations are taken into account in such a way that individual molecular blocks within the $(creat)_2CuCl_4$ crystal are treated as semi-rigid entities while the mutual positions of these blocks are subject to strong relative displacements. Creatinium tetrachlorocuprate $(creat)_2CuCl_4$ thus presents an example of a system where the effects of vibrations are significant at room temperature already within the first hundred eV.

Our results suggest that, whenever one observes different damping rates of XAFS oscillations for different polarizations, the presence of atomic pair-selective vibrations should be considered. Special attention should be given in this respect to systems where the interatomic distances can be split into different classes according to their presumed stiffness.

Atomic vibrations can be efficiently incorporated into XANES calculations by modifying the free-electron propagator *via* a damping factor, $G^{pq}_{LL'} \rightarrow G^{pq}_{LL'} \exp(-k^2\sigma^2_{pq})$. If this procedure is used, the effects of vibrations are treated within

the same approximations that are involved in the standard EXAFS formula while the multiple scattering itself is treated exactly.

Acknowledgements

This work was supported by the LD-COST CZ program of the Ministry of Education, Youth and Sport of the Czech Republic within the project LD15097. Stimulating discussions with P. Pattison are gratefully acknowledged.

References

Ahmed, S. I., Dalba, G., Fornasini, P., Vaccari, M., Rocca, F., Sanson, A., Li, J. & Sleight, A. W. (2009). *Phys. Rev. B*, **79**, 104302.
Benfatto, M., Natoli, C. R. & Filipponi, A. (1989). *Phys. Rev. B*, **40**, 9626–9635.
Beni, G. & Platzman, P. M. (1976). *Phys. Rev. B*, **14**, 1514–1518.
Bianconi, A., Li, C., Campanella, F., Longa, S. D., Pettiti, I., Pompa, M., Turtù, S. & Udron, D. (1991). *Phys. Rev. B*, **44**, 4560–4569.
Bocharov, S., Kirchner, T., Dräger, G., Šipr, O. & Šimůnek, A. (2001). *Phys. Rev. B*, **63**, 045104.
Bridges, F., Keiber, T., Juhas, P., Billinge, S. J. L., Sutton, L., Wilde, J. & Kowach, G. R. (2014). *Phys. Rev. Lett.* **112**, 045505.
Calandra, M., Rueff, J. P., Gougoussis, C., Céolin, D., Gorgoi, M., Benedetti, S., Torelli, P., Shukla, A., Chandesris, D. & Brouder, C. (2012). *Phys. Rev. B*, **86**, 165102.
Chaboy, J., Muñoz-Páez, A. & Sánchez Marcos, E. (2006). *J. Synchrotron Rad.* **13**, 471–476.
Cicco, A. D. (2003). *GNXAS*, http://gnxas.unicam.it.
Dimakis, N. & Bunker, G. (1998). *Phys. Rev. B*, **58**, 2467–2475.
Dimakis, N., Mion, T. & Bunker, G. (2009). *J. Phys. Conf. Ser.* **190**, 012011.
Filipponi, A., Di Cicco, A. & Natoli, C. R. (1995). *Phys. Rev. B*, **52**, 15122–15134.
Fornasini, P. & Grisenti, R. (2015). *J. Synchrotron Rad.* **22**, 1242–1257.
Fujikawa, T., Rehr, J., Wada, Y. & Nagamatsu, S. (1999). *J. Phys. Soc. Jpn*, **68**, 1259–1268.
Gonze, X., Amadon, B., Anglade, P. M., Beuken, J. M., Bottin, F., Boulanger, P., Bruneval, F., Caliste, D., Caracas, R., Côté, M., Deutsch, T., Genovese, L., Ghosez, P., Giantomassi, M., Goedecker, S., Hamann, D. R., Hermet, P., Jollet, F., Jomard, G., Leroux, S., Mancini, M., Mazevet, S., Oliveira, M. J. T., Onida, G., Pouillon, Y., Rangel, T., Rignanese, G. M., Sangalli, D., Shaltaf, R., Torrent, M., Verstraete, M. J., Zerah, G. & Zwanziger, J. W. (2009). *Comput. Phys. Commun.* **180**, 2582–2615.
Guo, J., Ellis, D. E., Goodman, G. L., Alp, E. E., Soderholm, L. & Shenoy, G. K. (1990). *Phys. Rev. B*, **41**, 82–95.
Hahn, J., Scott, R., Hodgson, K., Doniach, S., Desjardins, S. & Solomon, E. (1982). *Chem. Phys. Lett.* **88**, 595–598.
Hayakawa, K., Fujikawa, T., Nakagawa, K., Shimoyama, I., Titts-worth, R., Schilling, P. & Saile, V. (2003). *Chem. Phys.* **289**, 281–289.
Hayakawa, K., Kato, K., Fujikawa, T., Murata, T. & Nakagawa, K. (1999). *Jpn. J. Appl. Phys.* **38**, 6423–6427.
Ivashkevich, L., Kuz'Min, A. Y., Kochubei, D., Kriventsov, V., Shmakov, A., Lyakhov, A., Efimov, V., Tyutuynnikov, S. & Ivashkevich, O. (2008). *J. Surf. Investig.* **2**, 641–645.
Kosugi, N. (2002). *Chemical Applications of Synchrotron Radiation*, edited by T. S. Sham, pp. 228–284. Singapore: World Scientific.
Kosugi, N., Kondoh, H., Tajima, H. & Kuroda, H. (1989). *Chem. Phys.* **135**, 149–160.
Kosugi, N., Yokoyama, T., Asakura, K. & Kuroda, H. (1984). *Chem. Phys.* **91**, 249–256.
Krack, M. (2005). *Hartwigsen–Goedeker-Hutter type pseudopoten-tials*, https://sourceforge.net/p/cp2k/code/HEAD/tree/trunk/potentials/Goedecker/abinit/pbe/.
Lee, P. A., Citrin, P. H., Eisenberger, P. & Kincaid, B. M. (1981). *Rev. Mod. Phys.* **53**, 769–806.
Loeffen, P. W. & Pettifer, R. F. (1996). *Phys. Rev. Lett.* **76**, 636–639.
Manuel, D., Cabaret, D., Brouder, C., Sainctavit, P., Bordage, A. & Trcera, N. (2012). *Phys. Rev. B*, **85**, 224108.
Natoli, C. R., Benfatto, M., Della Longa, S. & Hatada, K. (2003). *J. Synchrotron Rad.* **10**, 26–42.
Nesvizhskii, A. I., Ankudinov, A. L. & Rehr, J. J. (2001). *Phys. Rev. B*, **63**, 094412.
Poiarkova, A. V. & Rehr, J. J. (1999). *Phys. Rev. B*, **59**, 948–957.
Rega, N., Brancato, G., Petrone, A., Caruso, P. & Barone, V. (2011). *J. Chem. Phys.* **134**, 074504.
Rehr, J. J. (2013). *FEFF*, version 9. http://feffproject.org.
Rehr, J. J. & Albers, R. C. (2000). *Rev. Mod. Phys.* **72**, 621–654.
Rehr, J. J., Kas, J. J., Vila, F. D., Prange, M. P. & Jorissen, K. (2010). *Phys. Chem. Chem. Phys.* **12**, 5503–5513.
Schnohr, C. S., Kluth, P., Araujo, L. L., Sprouster, D. J., Byrne, A. P., Foran, G. J. & Ridgway, M. C. (2009). *Phys. Rev. B*, **79**, 195203.
Sipr, O. (1996–1999). *RSMS*. Institute of Physics AS CR, Prague, Czech Republic.
Smith, T., Penner-Hahn, J., Berding, M., Doniach, S. & Hodgson, K. (1985). *J. Am. Chem. Soc.* **107**, 5945–5955.
Tanimizu, M., Takahashi, Y. & Nomura, M. (2007). *Geochem. J.* **41**, 291–295.
Udupa, M. & Krebs, B. (1979). *Inorg. Chim. Acta*, **33**, 241–244.
Vedrinskii, R. V., Kraizman, V. L., Novakovich, A. A., Demekhin, P. V. & Urazhdin, S. V. (1998). *J. Phys. Condens. Matter*, **10**, 9561–9580.
Veronesi, G., Degli Esposti Boschi, C., Ferrari, L., Venturoli, G., Boscherini, F., Vila, F. D. & Rehr, J. J. (2010). *Phys. Rev. B*, **82**, 020101.
Vila, F. D., Rehr, J. J., Rossner, H. H. & Krappe, H. J. (2007). *Phys. Rev. B*, **76**, 014301.
Vvedensky, D. D. (1992). *Unoccupied Electronic States*, edited by J. C. Fuggle and J. E. Inglesfield, pp. 139–176. Berlin: Springer.
Wu, Z. Y., Xian, D. C., Hu, T. D., Xie, Y. N., Tao, Y., Natoli, C. R., Paris, E. & Marcelli, A. (2004). *Phys. Rev. B*, **70**, 033104.
Yokoyama, T., Kosugi, N. & Kuroda, H. (1986). *Chem. Phys.* **103**, 101–109.
Yokoyama, T. & Ohta, T. (1996). *J. Phys. Soc. Jpn*, **65**, 3909–3914.
Yokoyama, T., Yonamoto, Y. & Ohta, T. (1996). *J. Phys. Soc. Japan*, **65**, 3091–3908.